

NONLOCAL DAMAGE THEORY

By Gilles Pijaudier-Cabot,¹ S. M. ASCE and Zdeněk P. Bažant,² F. ASCE

ABSTRACT: In the usual local finite element analysis, strain softening causes spurious mesh sensitivity and incorrect convergence when the element is refined to vanishing size. In a previous continuum formulation, these incorrect features were overcome by the imbricate nonlocal continuum, which, however, introduced some unnecessary computational complications due to the fact that all response was treated as nonlocal. The key idea of the present nonlocal damage theory is to subject to nonlocal treatment only those variables that control strain softening, and to treat the elastic part of the strain as local. The continuum damage mechanics formulation, convenient for separating the nonlocal treatment of damage from the local treatment of elastic behavior, is adopted in the present work. The only required modification is to replace the usual local damage energy release rate with its spatial average over the representative volume of the material whose size is a characteristic of the material. Avoidance of spurious mesh sensitivity and proper convergence are demonstrated by numerical examples, including static strain softening in a bar, longitudinal wave propagation in strain-softening material, and static layered finite element analysis of a beam. In the last case, the size of the representative volume serving in one dimension as the averaging length for damage must not be less than the beam depth, due to the hypothesis of plane cross sections. It is also shown that averaging of the fracturing strain leads to an equivalent formulation, which could be extended to anisotropic damage due to highly oriented cracking.

INTRODUCTION

Progressive damage due to distributed cracking has to be treated in structural analysis as strain softening. This behavior is typical of concrete and is observed also in many other brittle heterogeneous materials such as rocks, stiff clays, two-phase ceramics, various composites, ice, wood and wood particle board, paper, filled elastomers, polymers and asphalt concretes, fiber-reinforced concrete, etc. Strain softening can be modeled by various types of constitutive laws, including endochronic theory, plastic-fracturing theory, plasticity with decreasing yield limit, bounding surface theory, and most recently continuum damage theory (4).

Application of these models in finite element programs and other methods of structural analysis, however, runs into severe difficulties. As shown rigorously already in 1974 (2), when the stress-strain diagram exhibits a negative slope, and more generally when the matrix of tangential moduli ceases to be positive definite, the strain-softening damage tends to localize in a zone of vanishing volume (a line or a surface). This is true not

¹Grad. Res. Asst., Northwestern Univ., Evanston, IL 60201; on leave from Laboratoire de Mécanique et Technologie, Cachan, France.

²Prof. Dept. of Civ. Engrg., and Dir., Ctr. for Concrete and Geomaterials, Northwestern Univ. Tech 2410, Evanston, IL 60201.

Note. Discussion open until March 1, 1988. To extend the closing date one month, a written request must be filed with the ASCE Manager of Journals. The manuscript for this paper was submitted for review and possible publication on September 2, 1986. This paper is part of the *Journal of Engineering Mechanics*, Vol. 113, No. 10, October, 1987. ©ASCE, ISSN 0733-9399/87/0010-1512/\$01.00. Paper No. 21882.

only of statics, but also of dynamics (5,14,15). Because the energy dissipation per unit volume is finite, the vanishing of the damage zone volume causes the indicated structure to fail at zero energy dissipation. This is physically unrealistic, although mathematically the solutions of at least some structural problems with strain softening do exist and represent the limit of the finite element solution for a vanishing element size (4,5,8,10-12).

The consequence of strain localization due to strain softening is that finite element solutions exhibit strong spurious mesh sensitivity, becoming unobjective with regard to the analyst's choice of the mesh (2). These features have first been documented by numerical examples for simple strain-softening constitutive laws (4,8,9,11,16). Recently, however, it has been shown (12,13) by numerical examples of beams that the same spurious mesh sensitivity due to strain localization occurs with the models of continuum damage mechanics (17,26-28,33-38,40,46).

The simplest, but admittedly a crude method to avoid strain localization and the associated mesh sensitivity is to impose a lower limit on the element size (2), as introduced in the crack band model (8,9,11,16). Alternatively, a strain-softening band of a width that is a material property may be embedded in the finite elements, as is done in the composite damage models of Pietrusczak and Mróz (41), and Willam, et al. (44,45) (see also Ref. 4).

Still another possibility is to consider a line of damage (i.e., a crack), characterized by a stress-displacement rather than stress-strain relation, as developed for concrete in the model of Hillerborg, et al. (21,22). The line-crack stress-displacement formulation, however, is not generally applicable. It cannot cope with problems in which the damage zone does not localize fully, because the spacing of line cracks is arbitrary and makes the response of this model unobjective in such situations (4).

A more general and fundamental way to avoid strain localization to a zero volume and to overcome spurious mesh sensitivity is to adopt a nonlocal continuum approach (3,6,7,14). The idea of a nonlocal continuum, introduced during the 1960s by Kröner (29), Kunin (31), Krumhansl (30), Eringen and Edelen (19), and others (4), is to consider the stress to be a function of the mean of the strain from a certain representative volume of the material centered at that point. Introducing certain essential modifications of the classical nonlocal theory, Bažant, and Bažant, et al. (3,7,13) developed a nonlocal model that can handle strain softening in finite element analysis in a consistent manner, while at the same time avoiding spurious mesh sensitivity and precluding strain localization to a vanishing volume. The nonlocal formulation, which may be considered as the limit case of an imbricated system of finite elements (7,13), has nevertheless two properties that are inconvenient for practical applications: (1) The behavior is nonlocal for all situations, including the elastic or plastic-hardening response; and (2) an overlay with a local continuum must be introduced in order to avoid certain zero-energy periodic modes of instability. The objective of the present study is to develop a modified nonlocal formulation which avoids these two inconvenient properties.

To this end it is useful, although not requisite, to adopt a formulation in which damage is described by a separate variable, distinct from the variables that describe the elastic behavior. This convenient feature is

provided by continuum damage mechanics (17,25,27,28,33–37,40,46). The principal idea of this paper is to use the nonlocal concept only for the variables that control damage and not for the strains or stresses in the constitutive relation. Such an approach will represent a basic departure from the classical formulation of a nonlocal continuum.

The purpose of introducing the nonlocal concept for damage is to limit the localization of strain softening to a zone of a certain minimum size that is a material property, i.e., to serve as a localization limiter. A variety of mathematical formulations have recently been introduced to serve, in effect, as localization limiters. The simplest formulation of localization limiters is involved in the crack band model (2,8,9,11,16), as well as in the composite-damage finite element models (40,44,45). An alternative approach to localization limiters is to make the material strength or yield limit a function of the strain gradient. This idea, which was perhaps first proposed by L'Hermite and Grieu (32) for shrinkage cracking and was developed to describe the size effect in bending of concrete beams with assumed plane cross section (26), has recently been adopted for strain softening in general by Schreyer and Chen (43), Floegl and Mang (20), and Mang and Eberhardsteiner (39). Since the introduction of strain gradient is equivalent to comparing to the strength limit the stress value at a certain small distance from the point, this approach is also essentially nonlocal. Another variant of the nonlocal approach to localization limiters is to introduce into the constitutive equation higher-order spatial derivatives, particularly the Laplacian, which arise from a Taylor series expansion of the nonlocal averaging integral (3,1). In this study, which is based on a 1986 report (42), we will show that nonlocal damage is a very general and effective formulation of localization limiters.

CONTINUUM DAMAGE THEORY

For the sake of simplicity, attention will be restricted to isotropic materials with isotropic damage. Time-dependent material response (creep), as well as the effect of temperature and humidity will be neglected. The material will be assumed incapable of plastic behavior, which implies that unloading and reloading follow straight lines passing through the origin. Thus, our formulation of damage theory will be a special case of the general theory for continuum damage and plasticity (17,33). For the sake of simplicity, the anisotropic aspect of damage will be neglected, i.e., the general tensor Ω will be approximated by the spherical tensor $\Omega = \Omega \mathbf{I}$, where Ω is the scalar and \mathbf{I} the identity matrix. The present idea of nonlocal damage could nevertheless be implemented for anisotropic damage as well.

In the theory of continuum damage mechanics, first proposed by Kachanov (25) for creep and applied by Lemaitre, and Lemaitre and Chaboche (36,37), Krajcinovic (28) and others (17,40,46) to quasi-static behavior of strain-softening materials, the state of the material is characterized by strain tensor ϵ and damage Ω is evaluated at the given point of the continuum. The strains are assumed to be small. From the thermodynamic viewpoint, the state of the material may be characterized by its free energy density ψ , defined as

$$\rho\psi = \frac{1}{2}\sigma : \epsilon \dots\dots\dots (1)$$

in which ρ = mass density; the colon denotes the tensor product contracted on two indices; and σ = stress tensor, which may be expressed as

$$\sigma = \frac{\partial(\rho\psi)}{\partial\epsilon} \dots\dots\dots (2)$$

As a result of microcracking, the net resisting area of the material which transmits stress diminishes. Consequently the true stress σ' in the undamaged material between the cracks becomes larger than the macroscopic stress σ , which is in damage theory described by the relation (25):

$$\sigma' = \frac{\sigma}{(1 - \Omega)} \dots\dots\dots (3)$$

in which Ω = damage (we use Ω instead of the usual notation ω because Ω will be later defined as nonlocal while the notation ω is reserved for the usual local damage); Ω represents an internal (hidden) variable which can never decrease ($\dot{\Omega} \geq 0$), has the initial value $\Omega = 0$, and always $\Omega \leq 1$ with $\Omega = 1$ representing the idealized asymptotic failure of a homogeneously deformed material ($\epsilon \rightarrow \infty$, $\sigma \rightarrow 0$). In practice, failure occurs earlier, at $\Omega < 1$, which is obtained through analysis of localization, such as crack-tip singularity.

Assuming, for the sake of simplicity, that the strain in the undamaged matrix of the material is equal to the macroscopic strain, and that the material exhibits no plasticity, Lemaitre and Chaboche (38) and others expressed the true stress as

$$\sigma' = \mathbf{C} : \epsilon \dots\dots\dots (4)$$

Substituting Eq. 4 into Eq. 3, we have

$$\sigma = (1 - \Omega)\mathbf{C} : \epsilon \dots\dots\dots (5)$$

and substituting this into Eq. 1 we obtain

$$\rho\psi = \frac{1 - \Omega}{2} \epsilon : \mathbf{C} : \epsilon \dots\dots\dots (6)$$

Since damage comprises the creation and propagation of cracks and voids, growth of damage dissipates energy. By differentiation of Eq. 6, the energy dissipation rate is:

$$\varphi = -\frac{\partial(\rho\psi)}{\partial t} = -\frac{\partial(\rho\psi)}{\partial\Omega} \frac{\partial\Omega}{\partial t} = Y\dot{\Omega} \dots\dots\dots (7)$$

in which we introduce the quantity:

$$Y = -\frac{\partial(\rho\psi)}{\partial\Omega} = \frac{1}{2} \epsilon : \mathbf{C} : \epsilon \dots\dots\dots (8)$$

called the damage energy release rate (38). According to the second law of thermodynamics (or Clausius-Duhem inequality), $\varphi \geq 0$. Since Y is a positive definite function of ϵ and $\dot{\Omega} \geq 0$, this condition is always verified.

From this definition, however, one must exclude reverse stiffening phenomena such as crack healing. This phenomena could be described by a second damage variable (31,43).

The damage properties of the material may be generally characterized, on the basis of experiments, by the damage evolution equation of the form $\dot{\Omega} = f_1(\Omega, \epsilon; \sigma)$. Although the present idea can be applied in general, we will consider, for the sake of simplicity, only the special case where this evolution equation is integrable for monotonic damage growth and reduces to the functional form $\Omega = f(Y)$. Loading and unloading are distinguished by means of the loading function:

$$F(Y) = Y - \kappa(Y) \dots\dots\dots (9)$$

in which $\kappa(Y)$ = hardening-softening parameter. Its initial value is given as Y_1 . After Y first exceeds Y_1 , $\kappa(Y)$ is assumed to be equal to the largest value of Y reached thus far at the given point. The damage evolution at a point of the continuum for loading and unloading may then be defined as follows:

$$\text{If } F(Y) = 0 \text{ and } \dot{F}(Y) = 0, \text{ then } \dot{\Omega} = f(Y) \dots\dots\dots (10a)$$

$$\text{If } F(Y) < 0, \text{ or if } F(Y) = 0 \text{ and } \dot{F}(Y) < 0, \text{ then } \dot{\Omega} = 0 \dots\dots (10b)$$

It must be emphasized that Eqs. 5 and 8–10 serve only as a simple prototype of damage formulation. Obviously, more complicated damage evolution laws and damage loading functions are required to distinguish between damage in tension and compression, or in other triaxial states (33,46).

NONLOCAL CONTINUUM DAMAGE

The foregoing standard formulation of damage theory is local. It has been demonstrated (2,5–10,12,13) that, in a local theory, the damage or strain softening can, and often does, localize into a zone of vanishing volume. Since φ is finite, the total energy dissipation rate in this volume tends to zero, i.e.

$$\lim_{V \rightarrow 0} \int_V \varphi dV = 0 \dots\dots\dots (11)$$

In particular, the dynamic failure due to wave propagation in a material represented by the tensile stress-strain curve shown in Fig. 1(a) occurs right at the start of softening (i.e., at the maximum stress point), without any stable progressive accumulation of damage before failure and without any dissipation of energy (5). This physically unrealistic property is also borne out by numerical finite element computations when the finite element subdivision of the structure is refined (5,14). As already mentioned, it is proposed to circumvent this problem by defining damage in a nonlocal manner. This can be done by replacing the local definition, $\Omega = f(Y)$, with the nonlocal definition:

$$\Omega = f(\bar{Y}) \dots\dots\dots (12)$$

in which \bar{Y} represents the mean of Y over the representative volume V_r of the material centered around the given point and Ω the nonlocal damage.

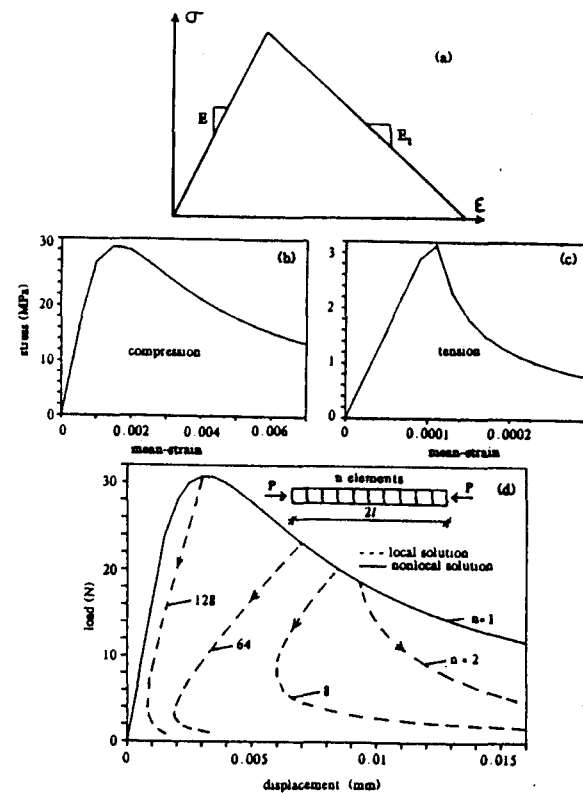


FIG. 1. (a) Simplified Triangular Stress-Strain Curve for Strain-Softening Materials; (b), (c) Stress versus Mean-Strain Curve for Nonlocal Model; (d) Local and Nonlocal Computation of Load-Displacement Curve in Compression

We will use

$$\bar{Y} = \frac{1}{V_r} \int_{V_r} Y dV \dots\dots\dots (13)$$

More generally, a weighting function could be introduced in the integrand of this equation, the same as in Ref. 3. The loading function for damage must also be formulated in terms of nonlocal quantities, i.e., Eq. 9 is replaced by

$$F(\bar{Y}) = \bar{Y} - \kappa(\bar{Y}) \dots\dots\dots (14)$$

and Y is replaced by \bar{Y} in Eq. 10. The representative volume in one, two, or three dimensions may be taken as a line segment of length l , or a circle or sphere of diameter l where l = characteristic length of the material. That spatial averaging becomes physically realistic if we note that the macroscopic equivalence between our assumed continuum with damage and the real heterogeneous material such as concrete cannot be achieved within a domain smaller than a few aggregate sizes. The material parameter l cannot be identified from tests of specimen whose strain is (or is assumed to be)

homogeneous. Identification of l will require both tests in which the damage localizes (as in fracture tests) and tests in which damage does not localize. This problem is beyond the scope of this paper.

Due to spatial averaging, a special treatment is required for points located at the boundary or so close to it that a part V^* of the material representative volume V_r protrudes outside the boundary. For such points, which occupy a boundary layer of a certain characteristic thickness that is a material property, Eq. 13 must be modified as

$$\bar{Y} = \frac{1}{(V_r - V^*)} \int_{V_r - V^*} Y dV \dots\dots\dots (15)$$

This means that the protruding part of the representative volume is chopped off and averaging is carried out only through the part of the representative volume that lies inside the body. The existence of a boundary layer is an inevitable consequence of the nonlocal continuum concept.

SPECIAL UNIAXIAL FORMULATION

In one dimension, the representative volume reduces to a line segment whose length is the characteristic length, l , provided that no weighting function is used. The mean damage energy release rate is defined as

$$\bar{Y}(x) = \frac{1}{(x_2 - x_1)} \int_{x_1}^{x_2} \frac{1}{2} E \epsilon^2(x) dx \dots\dots\dots (16)$$

where E = initial Young's elastic modulus. If the one-dimensional bar occupies the interval $0 \leq x \leq L$ such that $L > l$, the limits of the characteristic length are defined as

$$x_1 = x - l/2, x_2 = x + l/2 \quad \text{if } x_1 \geq 0; \quad \text{else } x_1 = 0, x_2 = x + l/2 \dots\dots\dots (17a)$$

$$x_1 = x - l/2, x_2 = x + l/2 \quad \text{if } x_2 \leq L; \quad \text{else } x_1 = x - l/2, x_2 = L \dots\dots\dots (17b)$$

The imbricate finite element scheme developed before to treat the nonlocal behavior could be chosen to calculate averages directly from nodal displacements. This approach, however, would be less efficient numerically since averaging, required only for computation of damage, can here be explicitly implemented with the usual, nonimbricated mesh on the basis of local strains.

To obtain a realistic shape of the stress-strain diagram with strain-softening, we use the following definition of damage evolution:

$$\text{If } F(\bar{Y}) = 0 \quad \text{and} \quad \dot{F}(\bar{Y}) = 0, \quad \text{then} \quad \Omega = 1 - \frac{1}{1 + b(Y - Y_1)^n} \dots\dots (18)$$

$$\text{If } F(\bar{Y}) < 0, \quad \text{or} \quad F(\bar{Y}) = 0 \quad \text{and} \quad \dot{F}(\bar{Y}) < 0, \quad \text{then} \quad \dot{\Omega} = 0 \dots\dots (19)$$

in which b , n , and Y_1 represent the material damage parameters, Y_1 being the damage threshold. In numerical computations, different thresholds, Y_1 , were used for tension and compression ($\sigma > 0$ or $\sigma < 0$). The parameters for tension were $b = 9.27 \times 10^{-3}$, $Y_1 = 180.5$ MPa, $n = 1$, and for compression $b = 2.05 \times 10^{-5}$, $Y_1 = 8540$ MPa, $n = 1$. Note that

generalization of Eq. 18 to multiaxial stress states would require certain precautions analyzed elsewhere (17,33).

It may be noted that, according to Eq. 18, the area under the complete uniaxial stress-strain diagram $\sigma = (1 - \Omega) E \epsilon$ up to $\epsilon \rightarrow \infty$ is infinite if $n = 1$, and finite if $n > 1$. For the modeling of complete failure due to distributed cracking, the stress-strain diagram should be integrable, however for the present purpose of demonstrating objectivity of the theory this condition is unimportant, and $n = 1$ has been used for the sake of simplicity. The formula in Eq. 18 for $n = 1$ has the advantage that its parameters b and E can be identified from given test data by linear regression if ϵ/σ is plotted versus $Y - Y_1$; the slope of the regression line of this plot is b/E , and its vertical axis intercept is $1/E$.

Obtained from Eq. 18, the stress versus mean strain (displacement divided by length) of a homogeneously deformed specimen of length l and a united cross-sectional area in tension and compression are shown Figs. 1(b) and (c). The shapes of these curves are obviously quite realistic for concrete.

To verify proper convergence of nonlocal damage formulation, various one-dimensional problems have been solved by finite elements. Only constant-strain finite elements have been used, for two reasons: (1) The numerical implementation of damage averaging is simpler than for higher-order elements; and (2) large higher-order elements cannot represent the discontinuities due to cracking as well as small constant-strain elements. The center of the averaging line segment having characteristic length l is made to coincide with the center of each element, whose coordinate is x^c . To implement the averaging, we need to first determine the numbers $n(i, j)$, $j = 1, \dots, n_e(i)$ of all finite elements which lie entirely or partly within the characteristic length l , and their total number $n_e(i)$. We also compute the portion $h_{i, j}$ of the element length h_e , which lies within the characteristic length, i.e., within the interval $(x_1^c - l/2, x_1^c + l/2)$, x_1^c being the coordinate of the center of the element number i . For elements that lie entirely within the characteristic length, $h_{i, j} = h_e$. At each loading step or time step of the computation, the mean value Y_i of Y is calculated for each element number i from the following averaging formula:

$$Y_i = \sum_{j=1}^{n_e(i)} \theta_{i, j} Y_{n(i, j)} \dots\dots\dots (20a)$$

$$a_i = \sum_{j=1}^{n_e(i)} h_{i, j} \dots\dots\dots (20b)$$

$$\theta_{i, j} = \frac{h_{i, j}}{a_i} \dots\dots\dots (20c)$$

which is applicable in general, whether or not the characteristic length reaches beyond the boundary. It is, of course, again advantageous to calculate the values of $h_{i, j}$ and a_i at the beginning of the computation and store them, provided that the computer's storage capacity is not overtaxed.

The averaging rule in Eqs. 20a-c has been implemented in a nonlinear finite element code based on continuum damage theory. First the tension

or compression of a bar consisting of N elements has been calculated for various element subdivisions of constant element size, with $N = 8, 64, 128$. The bar length is $L = 2l$ and the characteristic length is given as $l = 1$. For the nonlocal approach, calculated curves of stress versus mean strain in the bar are the same for various N [Figs. 1(b) and (c)]. For comparison, computations were also made for the classical local approach. In that case, it is found that at a certain point of the descending branch [the branching points in Fig. 1(d)], uniform deformation of the bar becomes unstable and further softening localizes into a single element whereas the other elements unload. The subsequent unstable portion of the response curve is numerically obtained by prescribing the strain into the softening element while the remaining part of the structure still behaves elastically. (According to Ref. 2, softening must localize into a single element if the formulation is local.) After the branching point (bifurcation point), only the response curve which descends sharply is possible. For sufficiently small elements, this curve exhibits snap-back [see Fig. 1(d); calculated for compression]. The fact that element subdivisions $N = 8, 64, 128$ give very different results confirms that local damage theory is unobjective with regard to element choice, i.e., it exhibits spurious mesh sensitivity and improper convergence, as established in Refs. 2 and 8. For the nonlocal solution [the smooth curve in Fig. 1(d)], no instability develops for this beam, which is relatively short compared to the characteristic length l . Note also that when the beam is loaded through a spring, which is typical of the situation in a testing machine, then instability (bifurcation) occurs earlier and the response curve after the critical point shifts to the left.

LONGITUDINAL WAVE IN STRAIN-SOFTENING MATERIALS

An instructive example to study dynamic strain localization due to strain softening is the interference of two longitudinal waves propagating in opposite directions (4). Consider a bar of length $L = 4l$, and beginning with the instant $t = 0$ we impose as the boundary conditions constant outward velocities $\dot{u} = -c$ at left boundary point $x = 0$ and $\dot{u} = c$ at right boundary point $x = L$ ($c > 0$). Velocities are such that the initial inward waves are elastic, consisting of a step of strain of magnitude $\epsilon = c/v$, where $v = (E/\rho)^{1/2}$ = elastic wave velocity and ρ = mass per unit length = 2,500 kg/m³. At time $t = L/2v$, the two elastic waves meet at midlength ($x = L/2$), which causes strain to instantly double if the behavior remains elastic. However, we assume the boundary velocities to be sufficiently large so that superposition of the two wave fronts at midlength would produce strain softening at the midlength point. In particular, we consider that c is such that $\epsilon = c/v = 0.75\epsilon_p$ (ϵ_p strain at peak stress).

For local behavior, this problem has an exact solution (5), which is unique and may be used for a convergence check of the finite element solution. We solve the problem with a uniform finite element subdivision, using both local and nonlocal damage models. The explicit algorithm, as stated in detail in Refs. 7 and 12, is used, with time step $\Delta t = 0.2 \times 10^{-6}$ sec. For numerical calculations we assume $Y_1 = 180.5$ MPa, $\epsilon_p = 10^{-4}$, $E = 32,000$ MPa, $c = 8.5$ mm/s.

Fig. 2 shows a comparison of nonlocal finite element solutions for different numbers N of finite elements with the exact local solution (5). A good

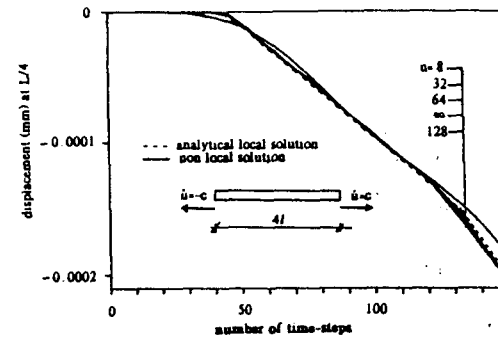


FIG. 2. Interference of Constant Strain Waves in Rod; Convergence of Displacements at $x = 1/4$

convergence may be noted. This is further apparent from Fig. 3, which shows the strain and stress histories at midlength for the nonlocal finite element solution, compared to the exact analytical solution. Despite large numerical noise, which is inevitable in this type of problem with a step wave front, the histories in Figs. 3(a) and (b) again indicate that convergence may be taking place for the overall response, the peak stress value excepted [Fig. 3(b)].

The profiles of strain ϵ and damage Ω at various times t are plotted in Figs. 4(a) and (b) for a mesh of $N = 64$ elements. The peak stress is reached [Fig. 3(b)] at time $t = 0.00185$ sec (93 time steps), and at $t = 0.0019$ sec (95 time steps) the damage has already started to develop and the strain profiles begin to exhibit a peak at midlength ($x = L/2$). It is noteworthy that the size (length) of the strain-softening zone is approximately equal to the characteristic length l . As it appears, l is the smallest length on which damage can exist [this observation lends further justification to the crack-band model (11)]. It may be also observed from the strain and damage profiles (Fig. 4) that the strain-softening zone gradually expands up to a size approximately $2l$. At the same time, damage accumulates within the entire strain-softening zone. Failure occurs for a high number of time steps in the damaged part of the bar.

The differences between local and nonlocal solutions are best revealed by Figs. 5(a)-(d). It shows the strain and damage profiles at time 3×10^{-5} sec for different numbers of elements, N . The strain profiles obtained for the local formulation [Fig. 5(b)] conspicuously display progressively sharper localization of the strain-softening damage zone, which apparently exhibits physically incorrect convergence to a Dirac delta function. By contrast, the nonlocal solution obviously converges [Figs. 5(a) and (c)] to a distribution with a finite-size strain-softening damage zone. This behavior is of the same type as previously achieved with the nonlocal imbricate continuum, in which the nonlocal concept was applied not only to damage but to total strains (7). The corresponding stress profiles are shown in Figs. 5(e) and (f), and again convergence to a strain-softening zone of finite size may be noted. The comparison in Fig. 5 provides the most compelling argument for the nonlocal approach to strain-softening damage.

In comparison to the previous nonlocal solution for the same problem based on the imbricate continuum model (7), it may be observed from the

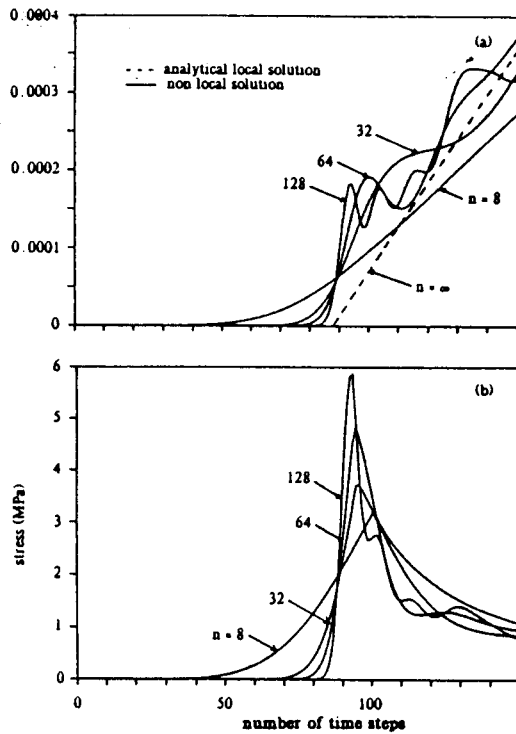


FIG. 3. Interference of Constant Strain Waves In Rod: (a), (b) Convergence of Stress and Strain Histories for Mesh Refinements

stress profiles at various times in Figs. 5(e) and (f) that the numerical solution behaves better near the boundary. In the previous solution, stress profiles near the boundary showed poor convergence, exhibited much numerical noise, and their boundary slopes were especially scattered. No doubt this was due to the difficulty in imposing physically reasonable boundary conditions when the total strain, including the elastic one, is treated in a nonlocal manner. In the present solution, characterized by local treatment of the elastic part of the strain, convergence and general behavior of the solution near the boundary is as good as it is in the interior of the bar.

The most important aspect of strain-softening damage is energy dissipation. According to Ref. 7 (Eq. 34), the total energy dissipated in the bar, W , may be calculated from the equation

$$W(t_{r+1}) = W(t_r) + \sum_{n=1}^N \frac{h_x}{2} \times [\sigma_{n,r} \epsilon_{n,r} - \sigma_{n,r+1} \epsilon_{n,r+1} + (\sigma_{n,r} + \sigma_{n,r+1})(\epsilon_{n,r+1} - \epsilon_{n,r})] \dots \dots \dots (21)$$

in which subscript n refers to element numbers and subscript r refers to discrete time t_r ($r = 1, 2, 3 \dots$). Fig. 6 shows the values of energy dissipated up to time $t = 3 \times 10^{-5}$ sec (150 time steps) for both local and nonlocal solutions. As before (7), we see that for the local solution, W

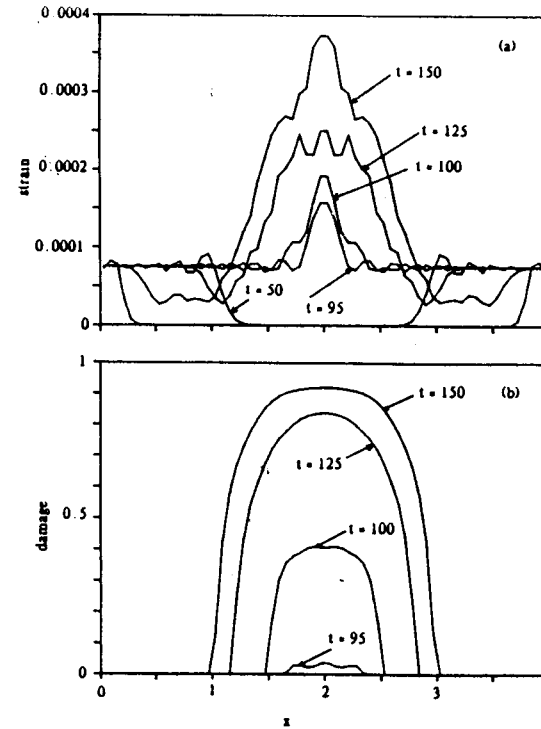


FIG. 4. Interference of Constant Strain Waves In Rod: (a), (b) Evolution of Strain and Damage Profiles

decreases as the number of elements N increases, and apparently converges to zero as $N \rightarrow \infty$. This property is physically unacceptable. By contrast, the present nonlocal solution, the same as the imbricate nonlocal solution in Refs. 7 and 10, yields about the same energy dissipation values for all element subdivisions and converges to a finite value as $N \rightarrow \infty$.

As another example (Fig. 7), we solve by finite elements a bar which is free at the left end ($x = 0$) and clamped at the right end ($x = L$). We assume that $L = 2l$. The boundary condition at $x = 0$ is $\sigma(t) = \sigma_0 H(t)$ where $H(t)$ is the Heaviside step function. At the right end, $u = 0$ at all times. Material properties are the same as in the previous example.

A wave with a step-function stress profile, with wave-front magnitude σ_0 , propagates toward the clamped end, and is reflected at time $t = L/v$, at which the stress is doubled according to the elastic solution. By choosing $\sigma_0 = 1.8$ MPa, the strain at wave arrival to the clamped end exceeds ϵ_p , and strain softening is produced at the clamped end.

For the local solution, strain-softening damage again does not propagate from the clamped end, i.e., it remains concentrated in a single element, the boundary element. Fig. 7(a) shows the histories of displacement u at bar midlength ($x = L/2$) for various element subdivisions N . The nonlocal solutions apparently converge as N increases. Fig. 7(b) shows the stress

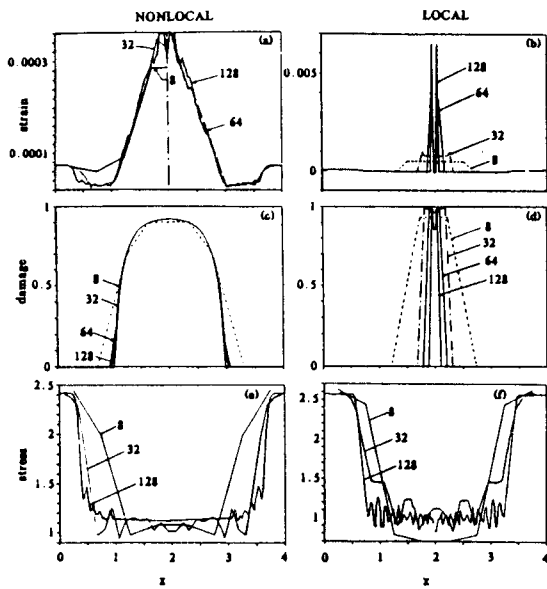


FIG. 5. Interference of Constant Strain Waves in Rod: (a) Convergence of Strain, (c) Damage and (e) Stress Profiles; (b), (d), (f) Comparison with Local Solution

history in the element at the clamped end for various N . Again, the nonlocal solution apparently converges, including peak stress value.

It may be noted that the present clamped bar responds overall in the same way as one-half of the bar in the previous example. However, comparison of Fig. 7(b) to Fig. 3(b) shows that for the same element size, peak stress values are different [4.7 MPa in Fig. 3(b) and 3.7 MPa in Fig. 7(b)], for element length 0.0625l.

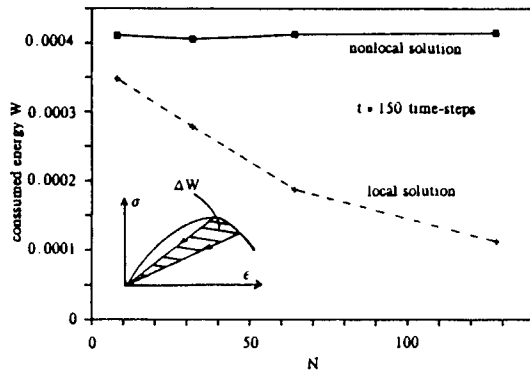


FIG. 6. Interference of Constant Strain Waves in Rod: Convergence of Energy Dissipated Due to Damage

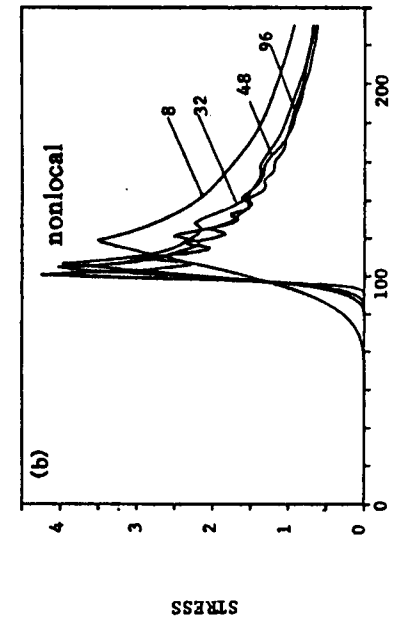
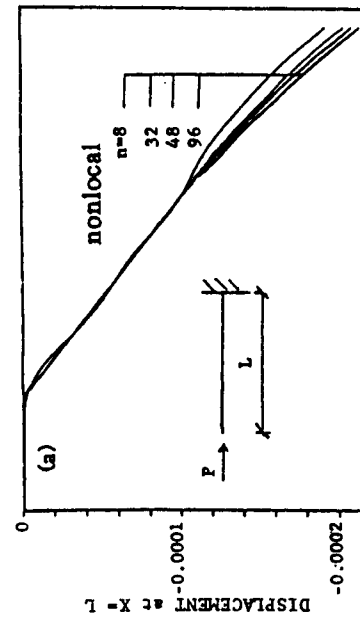
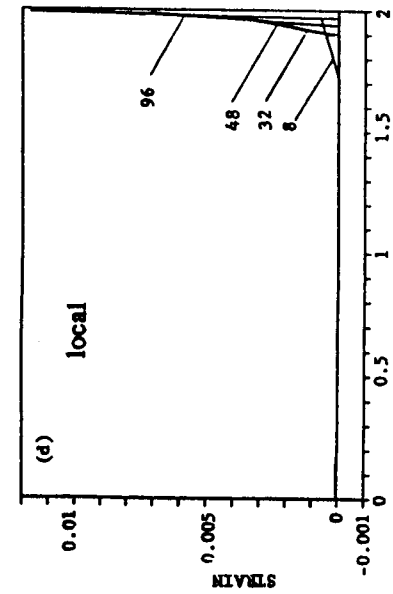
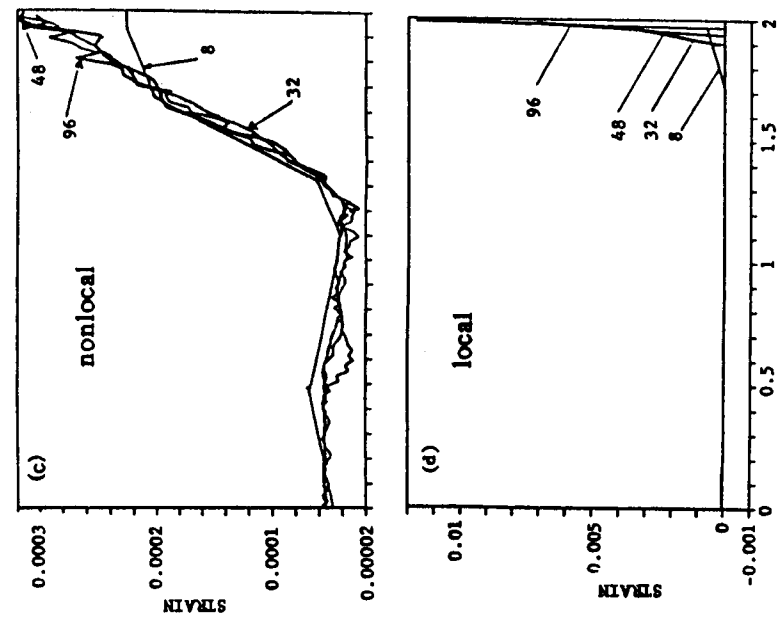


FIG. 7. Clamped Rod: Convergence of Displacements, (a), (b), (c) Stress Histories, and Strain Profiles for Mesh Refinements, (d) Comparison with Local Solution

Computations also showed [Fig. 7(d)] that convergence to finite unique values of u , ϵ , and σ is not achieved with the local formulation. Especially, the peak strain strongly depends on the element size.

STATIC PROBLEM OF BENDING THEORY

In a previous study (12,13) it was shown that solutions of beams and frames by the layered finite element technique also exhibit physically incorrect convergence and strong spurious sensitivity to element size when the material is assumed to exhibit strain softening and the formulation is local. Due to kinematic assumption of the preservation of planeness of cross sections and to Saint Venant's principle, the minimum length of finite elements is not only related to the characteristic length l of the material, but cannot be less than the beam depth h (12,13). This lower bound limitation on the element length may be directly used in a local-type finite element analysis similar to the multidimensional crack-band theory, in which a lower limit of the element size is imposed (2,8,11). With such a limitation, however, detailed stress and deflection distribution cannot be resolved, and numerical approximation is mathematically unfounded since the continuum limit at mesh refinement is left undefined.

This limitation may again be circumvented by the present concept of nonlocal damage. In the case of bending theory, however, the definition of spatial averaging (Eq. 6) must be slightly modified. Averaging length needs to be introduced as

$$l' = \max(l, h) \dots\dots\dots (22)$$

in which l is the previously introduced material characteristic length, and h = beam depth. For concrete, $l \approx 3d_a$ where d_a = maximum aggregate size, and since concrete beams are always deeper than three aggregate sizes, the beam depth limitation decides, i.e., $l' = h$. Thus, Eq. 16 for averaging of the damage energy release rate Y must be modified as

$$\bar{Y}(x, z) = \frac{1}{h} \int_{x-h/2}^{x+h/2} Y(\xi, z) d\xi, Y(\xi, z) = \frac{1}{2} B \epsilon^2(\xi, z) \dots\dots\dots (23)$$

in which x = length coordinate of the beam. Because damage localization in the vertical direction is impossible, due to the constraint of planeness of the cross section, we ignore averaging over the depth coordinate z . However, to take into account the well-known effect of strain gradient on the apparent strength or yield limit in concrete beams analyzed according to the bending theory (26), we could also introduce averaging over the depth:

$$\bar{Y}(x, z) = \frac{1}{hl} \int_{x-h/2}^{x+h/2} \int_{z-l/2}^{z+l/2} Y(\xi, \zeta) d\zeta d\xi \dots\dots\dots (24)$$

In the present study, which is concerned only with numerical problems of convergence and not with material properties, only the one-dimensional averaging in Eq. 23 has been used. Needless to elaborate, when the averaging length h (or l) protrudes beyond the boundary of the beam, the same treatment as before must be used (i.e., the averaging domain outside the beam is ignored). In the layered finite element model, Eq. 23 is applied

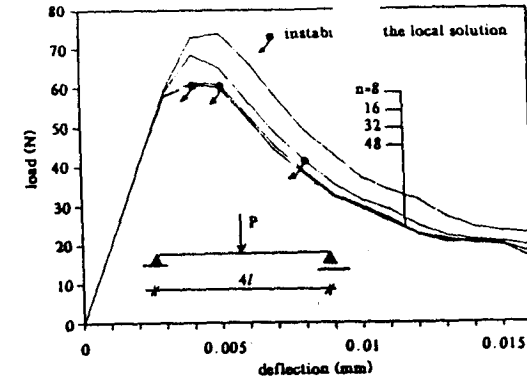


FIG. 8. Three-Point Bending; Convergence of Nonlocal Solution for Load-Deflection Curve

to each layer of each beam element, Y being assumed constant within each layer.

For demonstration, we solve one of the examples previously analyzed in Refs. 12 and 13. It is a simply supported beam of length $4h$, with a concentrated load at midspan (Fig. 8) and a square cross section. Material properties are the same as in our previous examples. Each beam element is divided into 10 layers. Step-by-step loading technique is used, with a load-point displacement controlled (prescribed) and the load calculated as a reaction. The direct iteration method based on the secant modulus is used (12,13). Numerical results for the load-displacement curve of the beam are plotted in Fig. 8 for various numbers N of elements along the beam, which all have the same length. We see that the solution converges well. By contrast, the local solution (12,13) showed a strong dependence on the number of elements N and produced instabilities of the snap-back type in the post-peak response, as discussed in Ref. 13. The occurrence of these instabilities depended on element size, not on beam properties. In the present solution, snap-back instability can occur only as a function of the L/h ratio, when its value is sufficiently high.

ALTERNATIVE VIEWPOINT: MEAN FRACTURING STRAIN

Among various possibilities of spatial averaging that do not affect elastic strain, another is to average the fracturing strain. This strain, imagined to represent the cumulative overall contribution of microcrack openings, was used as the basis of the crack band model (11) and similar formulations (41,44,45). The use of fracturing strain offers a simpler alternative to anisotropic damage in which the oriented aspect of damage due to cracking can be taken into account. Assuming all cracks to be parallel and denoting their normal direction as z , we write:

$$\epsilon_z = \epsilon_z^{e1} + \bar{\epsilon}_z^{fr} \dots\dots\dots (25a)$$

$$\bar{\epsilon}_z^{fr} = \frac{\sigma_z}{E} (1 + \bar{\gamma}) \dots\dots\dots (25b)$$

in which $\epsilon_z^{el} =$ elastic strain determined from stresses σ_x , σ_y , and σ_z and $\bar{\epsilon}_z^f =$ mean fracturing strain in the z -direction, specified as a function of strain (possibly also stress and internal variable), and $\bar{\gamma} =$ mean specific fracturing strain. Strains ϵ_y and ϵ_x in the directions parallel to the crack are elastic. According to the basic idea advanced here, $\bar{\gamma}(x)$ is obtained by spatial averaging:

$$\bar{\gamma}(x) = \frac{1}{l} \int_{-l/2}^{l/2} \gamma(x+s) ds \quad \dots \dots \dots (26)$$

By choosing

$$\gamma(x) = \left(\frac{b}{2} E \epsilon_x^2 \right)^n \quad \text{for loading} \quad \dots \dots \dots (27a)$$

$$\gamma = 0 \quad \text{for unloading and reloading} \quad \dots \dots \dots (27b)$$

the formulation becomes in one dimension identical to the foregoing damage model (Eq. 16). Indeed the damage model used in our examples yields for monotonic loading (and constant E) the uniaxial stress-strain relation

$$\sigma(x) = \frac{E \epsilon(x)}{1 + \left\{ \frac{b}{2l} E \int_{-l/2}^{l/2} [\epsilon(x+s)]^2 ds \right\}^n} \quad \dots \dots \dots (28)$$

and Eqs. 25–27 reduce for uniaxial stress to the same equation. By contrast, the classical local approach is equivalent, for monotonic loading, to the stress-strain relation

$$\sigma(x) = \frac{E \epsilon(x)}{1 + \left[\frac{b}{2l} E \epsilon^2(x) \right]^n} \quad \dots \dots \dots (29)$$

Alternatively, if the expression of the mean fracturing strain $\bar{\gamma}$ is a linear function of ϵ , averaging $\bar{\gamma}$ is equivalent to averaging the total strain ϵ , and so Eq. 28 is equivalent to:

$$\sigma(x) = \frac{E \epsilon(x)}{1 + \left\{ \frac{b}{2l} E \left[\int_{-l/2}^{l/2} \epsilon(x+s) ds \right] \right\}^{2n}} \quad \dots \dots \dots (30)$$

Fig. 9 shows for the dynamic example treated (Figs. 2–6), the result of this strain-averaging method. With the same overall material behavior, we find that the response diagrams are graphically undistinguishable from those obtained with the energy-averaging formulation.

Instead of Eq. 27, the expression for $\bar{\epsilon}_z^f$ may be taken as linear, which corresponds to the triangular stress-strain relation used in the original crack-band model [Fig. 1(a)]. By introducing the function $\gamma = \exp[-k\epsilon_z^n] - 1$ in which $k, n =$ constants, we obtain for $\sigma(x)$ a function which generalizes the local stress-strain relation $\sigma = E \epsilon \exp(-k\epsilon^n)$ also used in the past for the crack-band model.

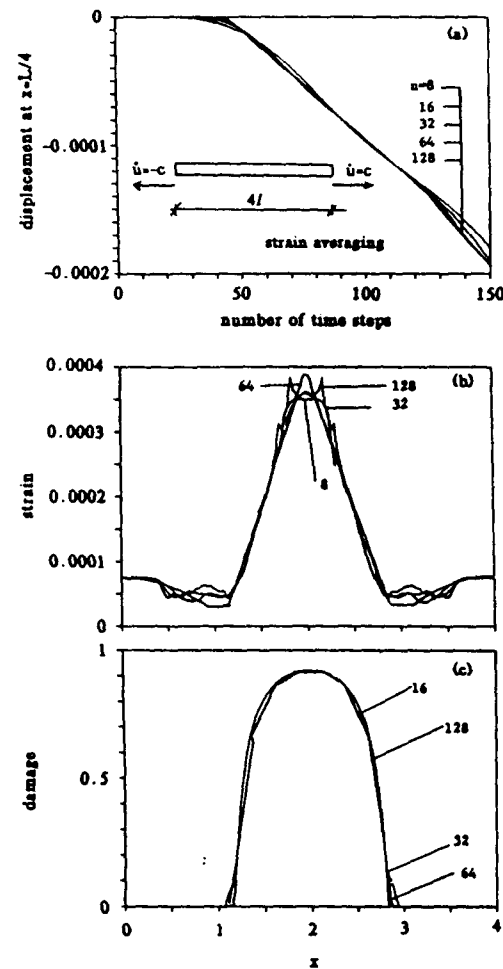


FIG. 9. Strain-Averaging Solution: (a) Convergence of Displacement History, (b), (c) Strain and Damage Profiles

Finally, we should comment on the failure mode. The true failure mode in tension no doubt consists of unstable (runaway) crack propagation. In the multiaxial analysis just illustrated, the transverse crack propagation cannot be modeled; however, by ensuring that $l(\int \sigma d\epsilon) =$ fracture energy of the material, our approach is equivalent to the fracture mechanics approach at least in the sense of total energy balance, which is most important. In local continuum softening analysis, energy balance is incorrect as dissipated energy vanishes. Compression failures can be described by our uniaxial analysis only to the extent that $l(\int \sigma d\epsilon)$ approximates the energy dissipated by axial splitting and shear cracks localized into a segment of specimen length. Such localization can occur only in long

compression specimens. A detailed analysis of compression failure must, of course, be three-dimensional.

CONCLUSIONS

1. Although existing imbricate nonlocal formulation for strain-softening materials does insure proper convergence and eliminates spurious mesh sensitivity, it has two inconvenient features: (1) All the behavior is formulated as nonlocal, including the elastic part of strain; and (2) an overlay with a local continuum must be introduced to suppress certain periodic zero-energy modes. These inconveniences are circumvented by the present nonlocal damage theory.

2. The key idea is that nonlocal treatment should be applied only to those variables that cause strain softening, and *not* to the elastic behavior. Thus, nonlocal theory should reduce to a local theory when the response is purely elastic. (The treatment of the plastic-hardening part of the response could no doubt also be local if this is convenient to do).

3. Among various constitutive models which can describe strain softening, the continuum damage mechanics appears ideal for the present purpose since all strain softening is controlled by a single variable, the damage. The essential attribute of the presently proposed nonlocal damage theory is that the damage energy release rate is averaged over the representative volume of the material whose size is a characteristic of the material. However, an alternative formulation in which spatial averaging is applied to the fracturing part (i.e., damage part) of the strain works equally well and may be just as efficient.

4. The characteristic length l (size of the representative volume) is a material property which must be determined by experiments and should be corroborated by micromechanics methods. No doubt, length l is related to the size of material inhomogeneities. However, when nonlocal damage theory is applied to beams, the assumption of preservation of the planeness of cross section requires that the averaging length not be smaller than the beam depth.

5. Numerical finite element computations indicate that nonlocal damage theory avoids spurious mesh sensitivity and that the calculated distributions of strain, stress, damage, and displacement exhibit proper convergence as the finite element subdivision is refined. Most importantly, the energy dissipated due to strain-softening damage converges to a finite value, while for the usual local finite element codes with strain softening this energy converges to zero as the mesh is refined, which is physically meaningless and unrealistic.

6. Since averaging is required by the present theory only in those domains of the structure that exhibit strong nonlinear behavior, the computation is more efficient than with previous imbricate nonlocal formulations. Averaging of damage can be easily introduced in any nonlinear finite element code with a strain-softening model.

ACKNOWLEDGMENTS

Partial financial support under U.S. Air Force Office of Scientific Research contract number F49620-87-C-0030DEF with Northwestern Uni-

versity, monitored by Spencer T. Wu, is gratefully acknowledged. Nadine Pijaudier-Cabot is thanked for her outstanding secretarial assistance.

APPENDIX I. REFERENCES

1. Aifantis, E. C., "On the Microstructural Origin of Certain Inelastic Models," *Journal of Engineering Materials Technology*, Vol. 106, 1984, pp. 326-330.
2. Bažant, Z. P., "Instability Ductility and Size Effect in Strain-Softening Concrete," *Journal of the Engineering Mechanics Division*, ASCE, Vol. 102, No. EM2, 1976, pp. 331-344; discussions Vol. 103, pp. 357-358, 775-777; Vol. 104, pp. 501-502 (based on Struct. Eng. Report No. 74-8/640, Northwestern University, August, 1974).
3. Bažant, Z. P., "Imbricate Continuum and Its Variational Derivation," *Journal of the Engineering Mechanics Division*, ASCE, Vol. 110, No. 12, 1984, pp. 1693-1712.
4. Bažant, Z. P., "Mechanics of Distributed Cracking," "Applied Mechanics Reviews", ASME, Vol. 39, No. 5, May, 1985, pp. 675-705.
5. Bažant, Z. P., and Belytschko, T. B., "Wave Propagation in a Strain-Softening Bar: Exact Solution," *Journal of the Engineering Mechanics Division*, ASCE, Vol. 111, No. 3, 1985, pp. 381-389.
6. Bažant, Z. P., and Belytschko, T. B., "Localization Limiters for Strain-Softening," Report No. 86-8/428L, Center for Concrete and Geomaterials, Northwestern University, Evanston, Il., August, 1986.
7. Bažant, Z. P., Belytschko, T. B., and Chang, T. P., "Continuum Theory for Strain-Softening," *Journal of the Engineering Mechanics Division*, ASCE, Vol. 110, No. 12, 1984, pp. 1666-1692.
8. Bažant, Z. P., and Cedolin, L., "Fracture Mechanics of Reinforced Concrete," *Journal of the Engineering Mechanics Division*, ASCE, Vol. 106, No. EM6, Dec., 1980, pp. 1287-1306; Discussion and Closure, Vol. 108, 1982, pp. 464-471; see also "Blunt Crack Band Propagation in Finite Element Analysis," *Journal of the Engineering Mechanics Division*, ASCE, Vol. 105, No. 2, 1979, pp. 297-315.
9. Bažant, Z. P., and Cedolin, L., "Finite Element Modeling of Crack Band Propagation," *Journal of Structural Engineering*, ASCE, Vol. 108, No. ST2, Feb., 1982.
10. Bažant, Z. P., and Chang, T. P., "Nonlocal Finite Element Analysis of Strain-Softening Solids," *Journal of the Engineering Mechanics Division*, ASCE, Vol. 113, No. 1, 1987, pp. 84-105.
11. Bažant, Z. P., and Oh, B. H., "Crack Band Theory for Fracture of Concrete," *Materials and Structures*, Vol. 16, No. 93, May-June, 1983, pp. 155-177.
12. Bažant, Z. P., Pan, J., and Pijaudier-Cabot, G., "Softening in Reinforced Concrete Beams and Frames," Report No. 86-7/428s, Center for Concrete and Geomaterials, Northwestern University, Evanston, Il., July, 1986.
13. Bažant, Z. P., Pijaudier-Cabot, G., and Pan, J., "Ductility, Size Effect and Redistribution in Softening Frames," Report No. 86-7/428d, Center for Concrete and Geomaterials, Northwestern University, Evanston, Il., July, 1986.
14. Belytschko, T. B., Bažant, Z. P., Hyun, Y. W., and Chang, T. P., "Strain-Softening Materials and Finite Element Solutions," *Computers and Structures*, Vol. 23, No. 2, 1986, pp. 163-180.
15. Belytschko, T. B., Wang, X., Bažant, Z. P., and Hyun, H., "Transient Solutions for One-Dimensional Problems with Strain-Softening," Report, Center for Concrete and Geomaterials, Northwestern University, Evanston, Il., June, 1986.
16. Cedolin, L., and Bažant, Z. P., "Effect of Finite Element Choice in Blunt Crack Band Analysis," *Computer Methods in Applied Mechanics and Engineering*, Vol. 24, No. 3, Dec., 1980, pp. 305-316.
17. Cordebois, J. P., "Critères d'instabilité plastique et endommagement ductile

- en grandes déformations," Thèse de Doctorat d'Etat ès Sciences Physiques, Université Paris VI, France, 1983.
18. De Borst, R., and Nauta, P., "Non-orthogonal Cracks in a Smearred Finite Element Model," *Engineering Computations*, No. 2, 1985, pp. 35-46.
 19. Eringen, A. C., and Edelen, D. G. B., "On Nonlocal Elasticity," *International Journal of Engineering Science*, Vol. 10, 1972, pp. 233-248.
 20. Floegl, H., and Mang, H. A., "On Tension-Stiffening in Cracked Reinforced Concrete Slabs and Shells Considering Geometric and Physical Nonlinearity," *Ingenieur-Archiv*, Vol. 51, No. 314, 1981, 215-242.
 21. Hillerborg, A., Modeer, M., and Petersson, P. E., "Analysis of Crack Formation and Crack Growth in Concrete by Means of Fracture Mechanics and Finite Elements," *Cement and Concrete Research*, Vol. 6, 1976, pp. 773-782.
 22. Hillerborg, A., "Numerical Methods to Simulate Softening and Fracture of Concrete," *Fracture Mechanics Applied to Concrete Structures*, edited by G. C. Sih, Martinus Nijhoff, The Hague, 1984.
 23. Ingraffea, A. R., "Fracture Propagation in Rock," *Mechanics of Geomaterials: Rocks, Concretes, Soils*, edited by Z. P. Bazant, Wiley, Chichester and New York, 1983, pp. 219-258.
 24. Ingraffea, A. R., *Fracture Mechanics Applied to Concrete Structures*, edited by G. C. Sih and A. Carpinteri, Martinus Nijhoff, The Hague, 1984.
 25. Kachanov, L. M., "Time of Rupture Process Under Creep Conditions" (in Russian), *Izvestia Akademii Nauk, USSR*, No. 8, 1958, pp. 26-31.
 26. Karsan, D., and Jirsa, J. O., "Behavior of Concrete Under Varying Strain Gradients," *Journal of Structural Mechanics Division*, ASCE, Vol. 96, No. ST8, 1970, pp. 1675-1696.
 27. Krajcinovic, D., and Fonseka, G. V., "The Continuous Damage Theory of Brittle Materials," *Journal of Applied Mechanics*, ASME, Vol. 48, Dec., 1981, pp. 809-815.
 28. Krajcinovic, D., "Constitutive Equations for Damaging Materials," *Journal of Applied Mechanics*, ASME, Vol. 50, Jun., 1983, pp. 355-360.
 29. Kröner, E., "Elasticity Theory of Materials with Longrange Cohesive Forces," *International Journal of Solids and Structures*, Vol. 3, 1968, pp. 731-742.
 30. Krumhansl, J. A., "Some Considerations of the Relations Between Solid State Physics and Generalized Continuum Mechanics," *Mechanics of Generalized Continua*, edited by E. Kröner, Springer-Verlag, Heidelberg, Germany, 1968, pp. 298-331.
 31. Kunin, I. A., "The Theory of Elastic Media with Microstructure and the Theory of Dislocations," *Mechanics of Generalized Continua*, edited by E. Kröner, Springer-Verlag, Heidelberg, Germany, 1968, pp. 321-328.
 32. L'Hermite, R., and Grieu, J. J., "Etude expérimentales récentes sur le retrait des ciments et des bétons," *Annales I.T.B.T.P. (Paris)*, Vol. 5, No. 52-53, 1952, pp. 494-514.
 33. Ladevèze, P., "On an Anisotropic Damage Theory" (in French), Internal Report No. 34, Laboratoire de Mécanique et Technologie, France, 1983.
 34. Leckie, F. A., "Constitutive Equations of Continuum Creep Damage Mechanics," *Philosophical Transactions of Royal Society, London*, Ser. A, Vol. 288, 1978, pp. 27-47.
 35. Leckie, F. A., and Onat, E. T., "Tensorial Nature of Damage Measuring Internal Variables," *Physical Nonlinearities in Structural Analysis*, edited by J. Hult and J. Lemaitre, Proceedings of the May, 1980, IUTAM Symposium Held at Senlis, France, Springer-Verlag, Berlin, 1981, pp. 140-155.
 36. Lemaitre, J., "How to Use Damage Mechanics" (Division lecture presented at SMiRT7, Chicago, 1983), Internal Report No. 40, Laboratoire de Mécanique et Technologie, Ecole Normale Supérieure de l'Enseignement Technique, Paris, France, 1983.
 37. Lemaitre, J., and Chaboche, J.-L., "Aspect phénoménologique de la rupture par endommagement," *Journal de Mécanique Appliquée (Paris)*, Vol. 2, 1978, pp. 317-365.
 38. Lemaitre, J., and Chaboche, J. L., "*Mécanique des matériaux solides*," Dunod-Bordas, Paris, 1985.
 39. Mang, H., and Eberhardsteiner, J., "Collapse Analysis of Thin R. C. Shells on the Basis of a New Fracture Criterion," *U.S.-Japan Seminar on Finite Element Analysis of Reinforced Concrete Structures*, Tokyo, May, 1985, Preprints, pp. 217-238.
 40. Mazars, J., "Application de la mécanique de l'endommagement au comportement non-linéaire et à la rupture du béton de structure," Thèse de Doctorat d'Etat ès Sciences Physiques, Université Paris VI, France, 1984.
 41. Pietruszczak, ST., and Mróz, Z., "Finite Element Analysis of Deformation of Strain-Softening Materials," Vol. 17, 1981, pp. 327-334.
 42. Pijaudier-Cabot, G., and Bažant, Z. P., "Nonlocal Damage Theory," Report No. 86-8/428n, Center for Concrete and Geomaterials, Northwestern University, Evanston, Il., August, 1986.
 43. Schreyer, H. L., and Chen, Z., "The Effect of Localization on the Softening Behavior of Structural Members," Proceedings of Symposium on Constitutive Equations: Micro, Macro, and Computational Aspects, ASME Winter Annual Meeting, New Orleans, Dec., 1984, edited by K. Willam, ASME, New York, 1984, pp. 193-203.
 44. Willam, K. J., Bicanic, N., and Sture, S., "Constitutive and Computational Aspects of Strain-Softening and Localization in Solids," Proceedings of Symposium on Constitutive Equations: Micro, Macro and Computational Aspects, ASME, Winter Annual Meeting, New Orleans, Dec., 1984, edited by K. J. Willam, ASME, New York, 1984.
 45. Willam, K. J., Hurlbut, B., and Sture, S., "Experimental, Constitutive and Computational Aspects of Concrete Failure," Preprints, *U.S.-Japan Seminar on Finite Element Analysis of Reinforced Concrete Structures*, Tokyo, May, 1985, pp. 149-172.
 46. Zaborski, A., "An Isotropic Damage Model for Concrete," (in French), Internal Report No. 55, Laboratoire de Mécanique et Technologie, E.N.S.E.T., Cachan, France, 1985.